

Geophysical Research Letters®



RESEARCH LETTER

10.1029/2024GL112212

Key Points:

- A rapidly-retreating marine-terminating glacier exported CH₄ to nearshore waters
- N₂O was undersaturated near the glacier front
- The regional CO₂ sink greatly outweighs CH₄ and N₂O emissions

Supporting Information:

Supporting Information may be found in the online version of this article.

Correspondence to:

Y. Y. Y. Yau,
yvonne.yau@gu.se

Citation:

Yau, Y. Y. Y., Cheung, H. L. S., Ljungberg, W., McKenzie, T., Henriksson, L., Majtényi-Hill, C., et al. (2025). Combined CH₄, N₂O, and CO₂ fluxes reveal a net carbon sink across a glacier-ocean continuum. *Geophysical Research Letters*, 52, e2024GL112212. <https://doi.org/10.1029/2024GL112212>

Received 30 AUG 2024

Accepted 16 JAN 2025

Author Contributions:

Conceptualization: Isaac R. Santos

Data curation: Henry L. S. Cheung

Formal analysis: Henry L. S. Cheung

Funding acquisition: Stefano Bonaglia, Isaac R. Santos

Investigation: Henry L. S. Cheung, Wilma Ljungberg, Tristan McKenzie, Linnea Henriksson, Claudia Majtényi-Hill, Isaac R. Santos

Methodology: Isaac R. Santos








Resources: Stefano Bonaglia

Supervision: Isaac R. Santos

Writing – review & editing: Henry

L. S. Cheung, Wilma Ljungberg, Tristan McKenzie, Linnea Henriksson, Claudia Majtényi-Hill, Stefano Bonaglia, Isaac R. Santos

Combined CH₄, N₂O, and CO₂ Fluxes Reveal a Net Carbon Sink Across a Glacier-Ocean Continuum

Yvonne Y. Y. Yau¹ , Henry L. S. Cheung¹ , Wilma Ljungberg¹ , Tristan McKenzie¹ , Linnea Henriksson¹ , Claudia Majtényi-Hill¹, Stefano Bonaglia¹ , and Isaac R. Santos¹ 

¹Department of Marine Sciences, University of Gothenburg, Gothenburg, Sweden

Abstract Rapidly retreating marine-terminating glaciers potentially release trapped greenhouse gases to the atmosphere. Here, we quantified water-air CH₄ and N₂O fluxes across a glacier-lagoon-ocean continuum in Iceland. Surface water CH₄ ranged from 690% supersaturation relative to atmospheric equilibrium near the glacier to 140% on the shelf. N₂O was undersaturated (84 ± 21%) near the glacier front and approached equilibrium in coastal seawater. The glacial lagoon was a CH₄ source to the atmosphere and N₂O sink, while nearshore shelf waters were a weak source of both gases. The total shelf CH₄ emissions to the atmosphere were one order of magnitude greater than the lateral freshwater dissolved CH₄ exports from the lagoon. The strong regional marine CO₂ sink exceeds the CO₂-equivalent global warming potentials of CH₄ and N₂O emissions to the atmosphere by one order of magnitude. Overall, the glacier-lagoon-shelf continuum remains a major carbon sink despite widespread CH₄ emissions and variable N₂O sink/source behavior.

Plain Language Summary Marine-terminating glaciers are retreating rapidly due to global warming. This study resolved greenhouse gas emissions from an Icelandic glacier front to continental shelf waters. We found waters highly enriched with methane near the glacier. Methane then decreased as the water flowed toward the open ocean. Nitrous oxide behaved differently with some areas near the glacier undersaturated. The glacial lagoon was a source of methane but a sink for nitrous oxide. The methane emitted from the coastal ocean was larger than the transport of glacier-sourced methane to the shelf. Yet, the ocean's strong ability to absorb carbon dioxide outweighed glacier-driven greenhouse gas emissions. Overall, high latitude coastal waters remain a strong net carbon sink.

1. Introduction

Rising ocean temperatures accelerate glacial retreat in polar regions (Tsubouchi et al., 2021). Marine-terminating glaciers, receiving heat from both atmospheric and marine sources, are particularly vulnerable to global warming (Kochitzky & Copland, 2022). Glacial discharge, entering the ocean via fjords, proglacial lakes, rivers, and lagoons, is important for land-ocean-atmosphere interactions (Hawkins, 2021). While increasing glacial discharge can enhance coastal organic matter fluxes (Overeem et al., 2017) and drive primary productivity (Meire et al., 2023), the influence of meltwater on greenhouse gas emissions remains poorly understood.

Glaciers and ice sheets could be a sink of carbon dioxide (CO₂) through chemical weathering and enhanced productivity (St. Pierre et al., 2019) or a source of CO₂ through microbial degradation of organic matter (Graly et al., 2017; Pain et al., 2021). Subglacial environments in Arctic and/or glacial-meltwater influenced environments are often enriched in dissolved CH₄ and N₂O (Manning et al., 2022; Pain et al., 2021; Rees et al., 2022; Schuler & Tortell, 2023). Better constraining CH₄ and N₂O emissions will improve the understanding of greenhouse gases emissions from retreating of glaciers.

Subglacial anoxic environments can produce CH₄ during remineralization of organic matter (Lamarche-Gagnon et al., 2019; Stibal et al., 2012). Aerobic CH₄ production has also been observed in Arctic waters (Damm et al., 2010; Repeta et al., 2016). Once formed, CH₄ could either be stored, oxidized, or exported through meltwaters, rivers, and emitted to the atmosphere. Active methanotrophs in subglacial environments can efficiently consume CH₄, limiting the release to the atmosphere (Sparrow et al., 2018; Stibal et al., 2012). Increasing glacier discharge accelerates the release of trapped CH₄ and N₂O (Wadham et al., 2019), and reshapes glacially-derived runoff via glacier-fed rivers, groundwater, and meltwaters (Burns et al., 2018; Kleber et al., 2023). This runoff can transport greenhouse gases to adjacent marine ecosystems (Damm et al., 2018; Verdugo et al., 2022).

© 2025. The Author(s).

This is an open access article under the terms of the [Creative Commons Attribution License](https://creativecommons.org/licenses/by/4.0/), which permits use, distribution and reproduction in any medium, provided the original work is properly cited.

Upwelling of subglacial discharge in marine-terminating glaciers supplies nutrients to surface waters (Meire et al., 2023) that may favor N_2O production.

Whilst previous work assessed greenhouse dynamics on polar shelf waters (Manning et al., 2022; Rees et al., 2022; Sparrow et al., 2018; Stroeve et al., 2014), few studies have explored how marine-terminating glaciers modify greenhouse gas fluxes at the land-ocean interface (Hopwood et al., 2020). Here, we investigate the impact of glacial meltwater on CH_4 and N_2O dynamics and water-air fluxes from a rapidly retreating marine-terminating glacier in Iceland (Jökulsárlón lagoon). We measured dissolved CH_4 and N_2O across the meltwater-lagoon-shelf continuum to discuss how the glacier impacts greenhouse gas emissions in a climate change hotspot.

2. Methods

2.1. Study Site

We performed expeditions to Jökulsárlón Lagoon (September 2022) and the adjacent continental shelf off Iceland (June 2023, Figure 1). The first expedition included onshore discrete sampling and time-series measurements within Jökulsárlón Lagoon, while the second focused on shore-perpendicular transects off Iceland's glacier-dominated southern coast using the R/V Skagerrak. Breiðamerkurjökull is a glacier outlet in southeast Iceland terminating in Jökulsárlón Lagoon, a rapidly-expanding proglacial coastal lagoon ($\sim 28 \text{ km}^2$, maximum depth 300 m) (Björnsson et al., 2001). The eastern side of the lagoon is shallow ($< 20 \text{ m}$), and fed by a glacial stream (Brandon et al., 2017). Jökulsárlón Lagoon connects to the North Atlantic Ocean through a well-mixed channel (6 m deep, 70 m wide) (Brandon et al., 2017). The lagoon experiences semi-diurnal tides with a tidal range of $\sim 0.95 \text{ m}$, alternating between saline Atlantic seawater and glacier meltwaters outflow (Brandon et al., 2017). The top 5 m of the lagoon is dominated by subglacial meltwater and remains ice-free year-round (Text S1 in Supporting Information S1). Sea surface temperature along Iceland's southern nearshore coast is around 8°C annually (Logemann et al., 2013). Heat from the warm seawater drives glacier melting, resulting in continuous export of freshwater (Brandon et al., 2017).

2.2. Experimental Approach

Surface waters in Jökulsárlón Lagoon including glacier front, as well as freshwater sources such as groundwater springs, glacial ponds, streams influenced by either groundwater or precipitation (clear), and glacier-fed rivers (milky) were sampled. Additionally, we also sampled glacier-fed rivers draining from Vatnajökull glacier. Discrete sampling was performed using a small motorboat. Water was sampled from groundwater springs, rivers, and the lagoon using a peristaltic pump or directly with syringes. We sampled for CH_4 and N_2O , water temperature, dissolved oxygen, and salinity using a handheld probe (YSI) and handheld CTD during lagoon survey (Figure S1 in Supporting Information S1). The nutrient and inorganic carbon cycle of the lagoon were recently reported in a companion paper (Ljungberg et al., 2024). All CH_4 and N_2O data reported here are original. Wind speeds were adjusted to 10-m height from the nearest weather station, Kvisker Vegagerðarstöð, 35315 (Amor-ocho & DeVries, 1980; IMO, 2024).

Time-series measurements were conducted at the lagoon mouth, $\sim 4 \text{ km}$ from the glacier front on 27th–30th September 2022. We measured water depth (Solinst), salinity (Solinst) and dissolved oxygen (miniDot Logger) every minute. Discrete samples of dissolved CH_4 and N_2O were collected every hour for 28 hr covering 2 full tidal cycles. Sampling on Iceland's southern continental shelf was conducted from the R/V Skagerrak (University of Gothenburg) across 6 shore-perpendicular transects (0–60 km offshore) (Figure 1). Water was collected from 3 m using the ship's internal pump with continuous data of water temperature, salinity, and oxygen from a Seabird Ferrybox system. Wind speed, corrected to 10 m, was obtained from the onboard weather system mounted $\sim 20 \text{ m}$ above sea level (Amor-ocho & DeVries, 1980, Texts in Supporting Information S1).

Dissolved CH_4 and N_2O were collected in 22 ml glass vials without headspace, preserved with 200 μl of ZnCl_2 and stored at 4°C (Thamdrup et al., 2019). Given the low concentrations of nitrite, ZnCl_2 preservation is not expected to significantly affect N_2O concentrations (Frey et al., 2024) (Text in Supporting Information S1). Gas concentration was determined using a N_2 headspace technique and gas chromatograph (Thermo Scientific Trace 1300) with flame ionization and electron capture detectors (Wilson et al., 2018). The instrument was calibrated with certified gas mixture of $50.1 \pm 1.0 \text{ ppm CH}_4$ and $4.69 \pm 0.23 \text{ ppm N}_2\text{O}$ (Air Liquide Gas AB). Laboratory

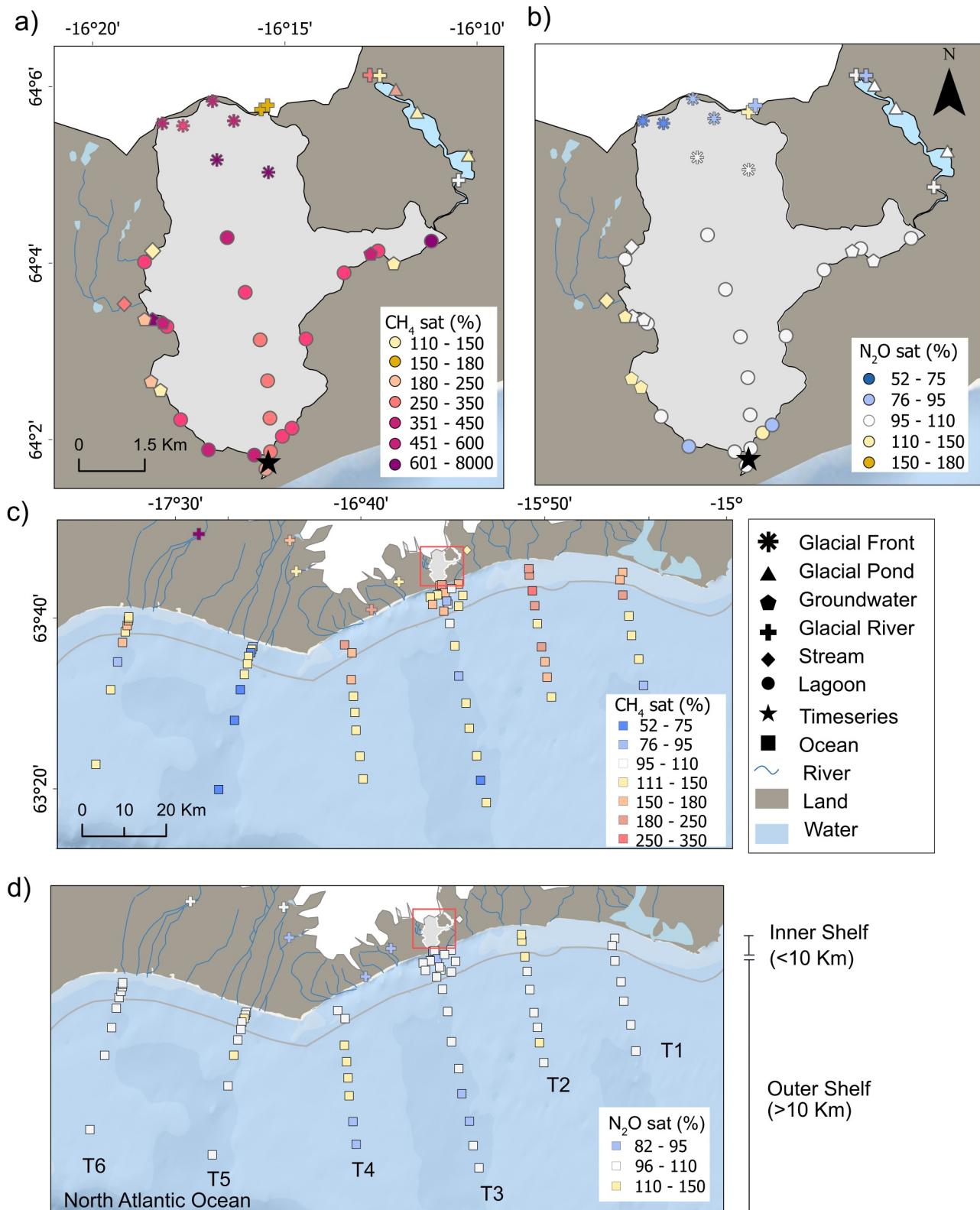


Figure 1. Sampling locations on Iceland's south coast. Surface water dissolved CH₄ and N₂O saturation (%) in Jökulsárlón Lagoon (a, b) and continental shelf receiving glacial meltwaters (c, d). Symbols represent different sample types. The glacier area was traced from Landsat 8 satellite images captured in December 2019 (USGS, 2019).

atmosphere air (1.9 ppm CH₄ and 0.339 ppm N₂O) was analyzed every 10 samples for drift correction. The detection limits were 0.06 ppm for CH₄ and 33 ppb N₂O with accuracy of ~99% from replicate measurements of standards. Nutrient (NO_x, NH₄) samples were filtered and measured with a flow injection analyzer (Seal analytical 2015) while dissolved organic carbon (DOC) was preserved with phosphorous acid and analyzed using a Shimadzu TOC-VCPH.

2.3. Calculations

CH₄ and N₂O saturation (% relative to air-equilibrated concentration) was calculated as the difference between measured dissolved concentrations and the calculated equilibrium concentration, which was derived from atmospheric air with temperature- and salinity-dependent solubility (Wiesenburg & Guinasso, 1979) (Text S1 in Supporting Information S1). The atmospheric CH₄ and N₂O was extracted from the global average averages of 1.9 ppmv and 334 ppbv, respectively (Lan et al., 2023). CH₄ and N₂O values are reported as % saturation to allow direct comparisons about their relative enrichments. Molar concentrations are shown in Supporting Information S1. Molar concentrations were calculated using the ideal gas law and solubility coefficients (Weiss & Price, 1980; Wiesenburg & Guinasso, 1979). Water-air flux was calculated using estimated gas transfer velocities (Wanninkhof, 2014) and the concentration difference between water and air.

The water discharge at the lagoon mouth was estimated from the relationship between water depth during timeseries measurements and current velocity collected at the same location under similar tidal amplitude during summer (Ljungberg et al., 2024; Þórarinnsson et al., 2020; Þórarinnsson & Hróðmarsson, 2022) (Text S1 in Supporting Information S1). No seasonal water flow observations are available for the lagoon. Lateral CH₄ and N₂O fluxes across the lagoon and ocean were calculated by multiplying the water discharge with the gas concentration at each time step and integrated over tidal cycles. The fluxes were then normalized to the lagoon area (Texts in Supporting Information S1). Freshwater discharge, combining surface runoff, subglacial runoff, and ice melt, was estimated by integrating the total water discharge and multiplying by the proportion of freshwater derived from a salinity mixing model (Brandon et al., 2017). Apparent oxygen utilization (AOU) was calculated from the air-saturated concentrations at the in situ temperature and salinity. Spearman correlations were used to explore the links between environmental variables. All statistical analyses were performed using R (R Core Team, 2021).

3. Results

3.1. Lagoon Spatial Survey and Glacial Endmembers

Lagoon water at the glacier front was colder (Table S1 in Supporting Information S1). CH₄ concentrations peaked at 27.5 nM (670%) near the glacier front and decreased to 10.9 nM (270%) toward the lagoon mouth (Figures 1a and 2b). All freshwater inputs, including glacial river, glacial pond and groundwaters were oversaturated with CH₄, ranging from 130% to 630% (Figure 2a, Table S2 in Supporting Information S1). The mean CH₄ saturation within the lagoon was $450 \pm 200\%$ (Table S1 in Supporting Information S1). The CH₄ hotspot area, affected by meltwater with CH₄ exceeding 20 nM, covered 20% of the lagoon area. CH₄ was negatively correlated with distance from coast (Figure S2 in Supporting Information S1) and DOC (Figures S3 and S4 in Supporting Information S1). The area-weighted mean water-air CH₄ flux was $26 \pm 19 \mu\text{mol m}^{-2} \text{d}^{-1}$, indicating the lagoon was a CH₄ source (Table S1 in Supporting Information S1).

N₂O displayed a contrasting spatial distribution (Figure 1b). N₂O was undersaturated ($84 \pm 21\%$) near the glacier front and approached equilibrium with the atmosphere at the lagoon mouth ($101 \pm 5\%$) (Table S1 in Supporting Information S1). The average lagoon N₂O saturation was $96 \pm 13\%$, indicating uptake from the atmosphere. Groundwater was the only source oversaturated in N₂O, while glacial ponds and glacial rivers were undersaturated or near equilibrium (Figure 2b). No significant correlation was observed between N₂O and dissolved oxygen in the lagoon (Figures S5 and S6 in Supporting Information S1). The area-weighted mean water-air N₂O fluxes in the lagoon approached zero ($-0.4 \pm 1.4 \mu\text{mol m}^{-2} \text{d}^{-1}$) with waters near the glacier representing a sink and waters near the ocean representing a source (Tables S1 and S6 in Supporting Information S1).

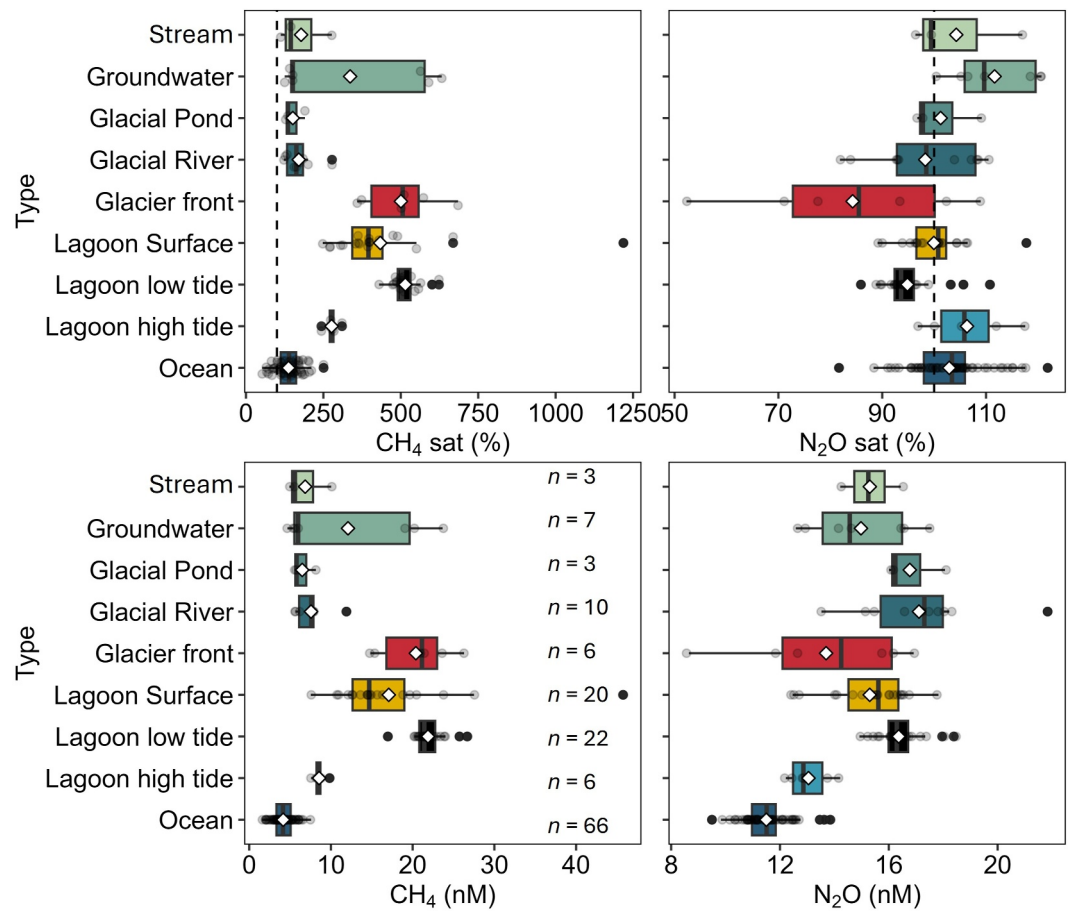


Figure 2. (a) CH₄ and N₂O saturation levels relative to atmosphere (%) and (b) concentration (nM) across different water types. The dashed line indicates 100% saturation. Box plot indicates median and 95% confidence intervals, gray dots are the individual sample point and the white diamond indicates mean. *n* represents the number of samples (Table S2 in Supporting Information S1).

3.2. Lagoon Mouth Time-Series

The time-series station at the mouth of the lagoon revealed rapidly changing conditions, with lagoon-dominated (ebb and low tide) and ocean-dominated (flood and high tide) periods (Figure 3). Glacial discharge was estimated at $20.2 \pm 9.7 \times 10^6 \text{ m}^3 \text{ d}^{-1}$ based on observed salinity and hourly flows. During the lagoon-dominated low tide, water temperature was 1.7°C , salinity was 9.6, dissolved CH₄ exceeded atmospheric equilibrium ($530 \pm 40\%$), and N₂O was slightly below equilibrium ($94 \pm 5\%$) (Table S3 in Supporting Information S1). As seawater flowed into the lagoon during the high tide, water chemistry drastically changed. Water temperature increased to 6.6°C , salinity rose to 30, and oxygen increased to 110% (Figure 3). Importantly, CH₄ saturations decreased by 34%, ²²²Rn decreased by 32%, and N₂O saturations increased by 12%. The net lateral export fluxes of CH₄ and N₂O from the glacier-fed lagoon to the coastal ocean were 760 ± 50 and $460 \pm 30 \text{ mol d}^{-1}$, respectively. Freshwater contributed 464 ± 245 and $266 \pm 145 \text{ mol d}^{-1}$, respectively (Table S4 in Supporting Information S1). These lagoon-ocean horizontal CH₄ and N₂O fluxes were comparable to the lagoon water-air vertical CH₄ fluxes.

3.3. Continental Shelf Transects

Lower seawater salinity and temperature just outside the glacial lagoon revealed a meltwater plume (Figures S7 and S8 in Supporting Information S1). CH₄ saturations rapidly decreased from the inner (210%) to the outer shelf (70%) (Figure 1). N₂O saturations were the lowest (80%) near the mouth of the glacier lagoon and increased further offshore, but did not exhibit a clear trend across all shelf transects (Figure 1, Figure S8 in Supporting Information S1). Both inner (<10 km from the shoreline) and outer (>10 km) shelf regions acted as sources of

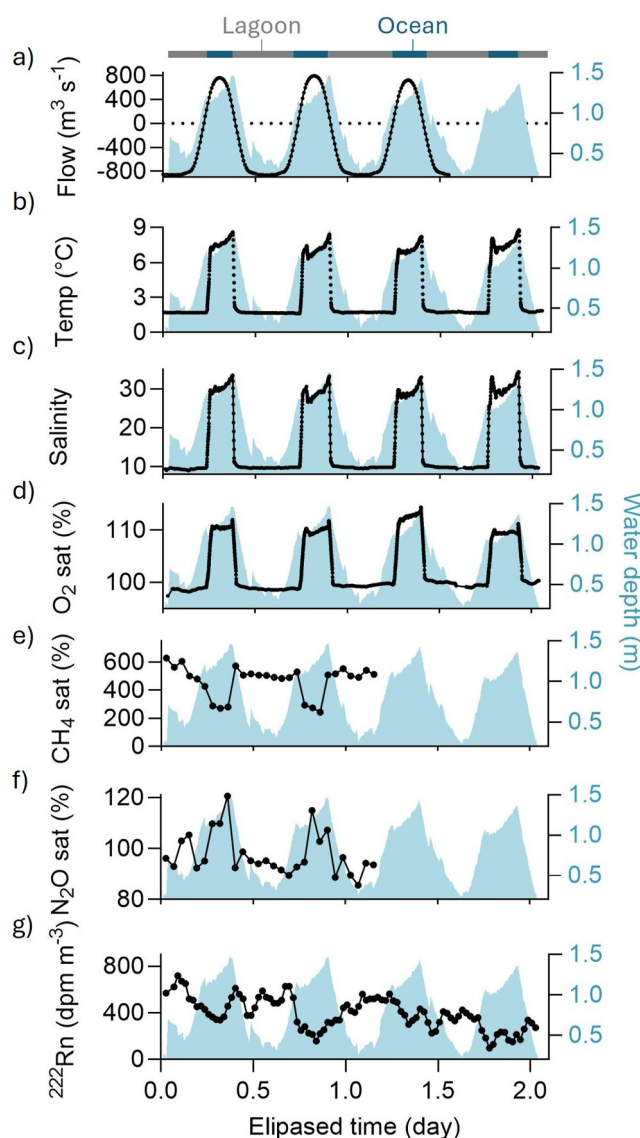


Figure 3. Time-series measurements at the glacier lagoon mouth reveal lagoon-ocean exchange. (a) water discharge, (b) water temperature, (c) salinity, (d) dissolved oxygen saturation, (e) CH_4 saturation, (f) N_2O saturation, and (g) radon concentration. Blue shaded area indicates water depth. Negative flow indicates water from lagoon flows to the ocean, and positive flow indicates seawater penetration into the lagoon. Ancillary data originally reported in Ljungberg et al. (2024). CH_4 and N_2O concentrations were sampled hourly for 2 complete tidal cycles.

CH_4 and N_2O to the atmosphere with area weighted fluxes of 1.3 ± 4.0 and $0.4 \pm 1.7 \mu\text{mol m}^{-2} \text{d}^{-1}$, respectively (Tables S5 and S6 in Supporting Information S1). The glacier-influenced nearshore plume had slightly higher CH_4 and lower N_2O fluxes. Across the glacier-ocean continuum, CH_4 saturation had a negative correlation with salinity (Figure S9 in Supporting Information S1) and distance to shore (Figure S10 in Supporting Information S1). DOC and NO_x had a positive but weak correlation with N_2O (Figure S9 in Supporting Information S1).

4. Discussion

4.1. Enhanced CH_4 Concentrations in Proximity of Meltwater

Supersaturated CH_4 near the glacial front, with a decreasing trend toward the lagoon mouth suggests the glacier environment or processes happening in sediments beneath the glacier as the primary CH_4 source. This is further supported by high CH_4 throughout the freshwater endmembers, including a glacial pond, glacial rivers, and

shallow groundwater (Figure 2). However, meltwater CH_4 concentrations (22 ± 5 nM) were four orders of magnitude lower than those recorded in the neighboring geothermally-influenced Sólheimajökull glacier (40–470 μM) (Burns et al., 2018) and one order of magnitude lower than subglacial runoff from the Greenland Ice Sheet (270 nM) (Lamarche-Gagnon et al., 2019). The relatively high CH_4 concentrations associated with low salinity and high radon at the lagoon mouth time series imply basal meltwater in contact with rocks, generating a radon signal. However, the high spatial variability in CH_4 concentration across glaciers require further investigation.

Our average glacier lagoon CH_4 saturations were comparable to surface waters in tidewater glaciers from other Arctic regions (Kleber et al., 2023; Rees et al., 2022; Schuler & Tortell, 2023). Lagoon CH_4 concentrations exceeding atmospheric equilibrium by 600% are comparable to surface water measurements in Greenland (450% saturation) (Crabeck et al., 2014) and Svalbard (Damm et al., 2005; Kleber et al., 2023) fjords. The negative relationship between CH_4 saturation with salinity and DOC along the glacier-ocean continuum (Figure S9 in Supporting Information S1) suggests that the glacial environment or processes beneath the glacier were the primary CH_4 source (as opposed to in situ production in the shelf). The mixing of meltwater with North Atlantic seawater diluted CH_4 values leading to small atmospheric fluxes ($1.3 \pm 4.0 \mu\text{mol m}^{-2} \text{d}^{-1}$) over the surveyed area (6800 km^2) (Table S6 in Supporting Information S1). Our CH_4 fluxes are comparable to mean CH_4 fluxes measured in the Northern Bering Sea, Eastern Chukchi Sea, Southern Beaufort Sea and Northwest Passage, ranging from 0.4–3.7 $\mu\text{mol m}^{-2} \text{d}^{-1}$ (Manning et al., 2022). Yet, CH_4 fluxes measured by eddy covariance in the Laptev and East Siberian Sea (109–286 $\mu\text{mol m}^{-2} \text{d}^{-1}$, Thornton et al., 2020) were two orders of magnitude higher than our shelf fluxes.

4.2. N_2O Source/Sink Behavior Across the Glacier-Ocean Continuum

N_2O exhibited a complex source-sink behavior across the glacier-ocean continuum. High N_2O concentration was detected in glacier river and glacier pond, coincided with elevated NO_x (Figure 2, Table S2 in Supporting Information S1). Similar N_2O concentrations were detected in multi-year sea ice in Baffin Bay (19.8 nM) and Canadian Archipelago (21 nM) (Kitidis et al., 2010). In the lagoon, N_2O was undersaturated near the glacier front potentially due to physical dilution and/or biological uptake. Dilution from mixing of freshwater within 200 m of the ice front could decrease N_2O saturation (Brandon et al., 2017) (Figure 1). Undersaturated N_2O has also been observed in glacier fjords in Chile (Fariás et al., 2018) and in subpolar Arctic waters influenced by sea ice melting (Fenwick et al., 2017; Randall et al., 2012; Rees et al., 2021; Zhang et al., 2015), suggesting that meltwater may reduce N_2O . Alternatively, biological N_2O consumption as observed in Icelandic surface waters (Rees et al., 2021) could contribute to N_2O undersaturation. Depending on the nitrate availability, N_2O consumption would require complete denitrification under low oxygen conditions.

N_2O levels occasionally exceeded saturation at the lagoon mouth and coastal ocean (Figures 1b, 1d, and 2). This increasing trend was also observed away from glacier fjord systems in Chile (Fariás et al., 2018). Similar concentration of N_2O (11.5 nM) was detected in North Atlantic Ocean near southern Iceland (Kitidis et al., 2010). The continental shelf of Iceland acted as a weak N_2O source, with mean water-air fluxes of $0.4 \pm 1.7 \mu\text{mol m}^{-2} \text{d}^{-1}$ (Table S6 in Supporting Information S1), consistent with observations in Nordic and Arctic Seas (Rees et al., 2022; Zhang et al., 2015), in contrast to the net N_2O sinks observed in the North Arctic Ocean (Manning et al., 2022). Further studies are needed to identify the mechanisms driving the N_2O source/sink behavior.

4.3. Net Global Warming Impact of CH_4 and N_2O Fluxes

The glacier-ocean continuum acted as a dynamic conduit for greenhouse gases. Our time series at the lagoon mouth revealed export of CH_4 and N_2O from glacier meltwater, resulting in enriched CH_4 and dilution of N_2O in shelf waters. With a freshwater discharge rate of $-20.2 \pm 9.7 \times 10^6 \text{ m}^3 \text{d}^{-1}$ integrated over complete tidal cycles, the freshwater from glacier lagoon laterally exported 464 ± 245 and $266 \pm 145 \text{ mol d}^{-1}$ of CH_4 and N_2O , respectively (Table S4 in Supporting Information S1). This first-order extrapolation from the timeseries measurements assumed similar flow discharge and gas fluxes during the two expeditions conducted toward the end of the summer melt season. Yet, the enriched CH_4 from glacial meltwater appears largely confined to the inner shelf, with a minor signal 20 km beyond the shoreline (Figures S8 and S10 in Supporting Information S1).

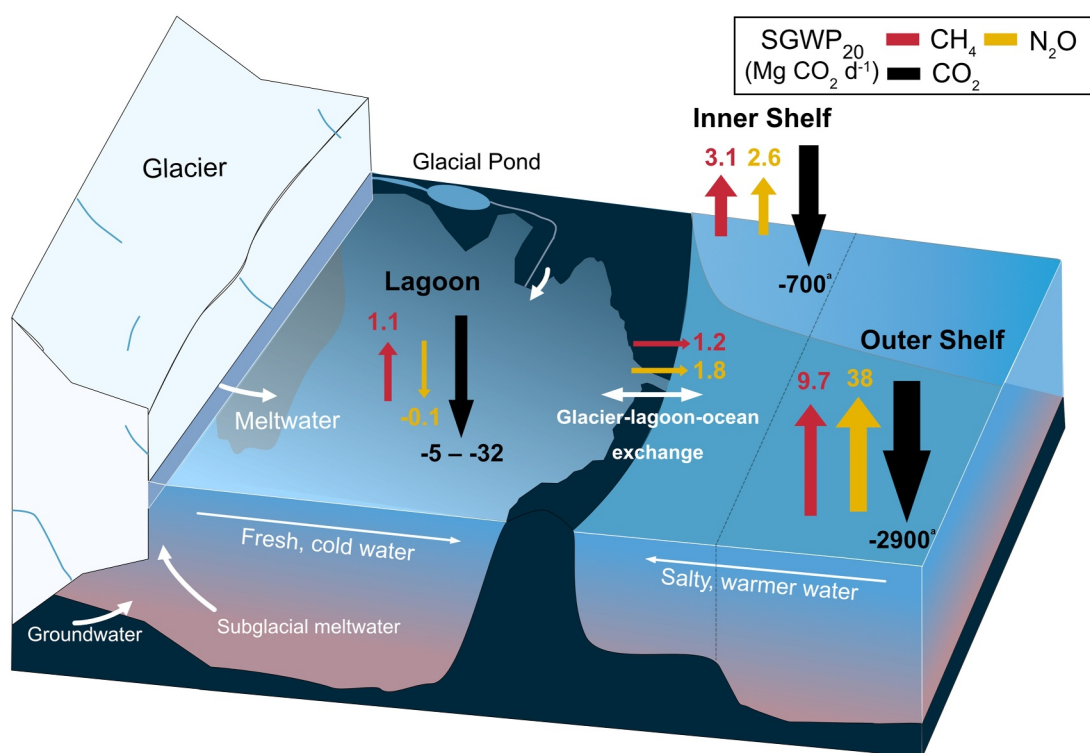


Figure 4. Schematic diagram summarizing CO₂-equivalent gas fluxes across Iceland's glacier-ocean interface. The arrows represent greenhouse gas sources (up) and sinks (down). Fluxes were converted to sustained global warming potential in 20 years (SGWP₂₀) by multiplying the mass-unit fluxes by a factor of 96 (Table S7 in Supporting Information S1) (Neubauer & Megonigal, 2019). The diagram was inspired by Hawkins (2021) and Ljungberg et al. (2024). ^aLagoon and shelf CO₂ fluxes were derived from Ljungberg et al. (2024) and Jeansson et al. (2015) (Tables S6 and S7 in Supporting Information S1).

To assess the regional contribution of CH₄ and N₂O air-sea fluxes, we calculated the total areal fluxes across the glacier-ocean continuum. The total sea-air CH₄ and N₂O fluxes from the studied continental shelf waters (6800 km²) were 0.15 ± 5.1 Mg CH₄ d⁻¹ and 0.04 ± 1.5 Mg N₂O d⁻¹, respectively, which was 13 times higher than the fluxes from the lagoon (Figure 4, Table S6 in Supporting Information S1). This first order extrapolation should be interpreted cautiously as fluxes were only obtained in the early autumn season. During summer, subglacial meltwater discharge into the lagoon is higher, primarily driven by enhanced glacial meltwater flow and increased surface melting of the glacier due to increasing air temperature (Brandon et al., 2017; Voytenko et al., 2015). Our measurements likely overestimate fluxes since they are conducted near the end of the peak meltwater season. During winter, lower meltwater discharge to the lagoon and higher seawater intrusion likely result in lower CH₄ fluxes as observed (Harris, 1976; Voytenko et al., 2015). Seasonal CH₄ and N₂O observations would be essential to refine budgets and extrapolations. The large shelf area magnifies small areal atmospheric fluxes into a much greater total water-air flux compared to the lagoon source. The total shelf vertical atmospheric CH₄ emissions ($9,100 \pm 24,400$ mol d⁻¹) were one order of magnitude greater than the lateral freshwater dissolved CH₄ exports from the lagoon (464 ± 245 mol d⁻¹) (Table S4 in Supporting Information S1), suggesting additional CH₄ sources, such as glacier rivers along the coast and aerobic methanogenesis in seawaters (Repeta et al., 2016; Sparrow et al., 2018).

Despite CH₄ emissions across the coastal continuum, the strong regional CO₂ uptake capacity creates a net sink for greenhouse gases. Our companion paper demonstrated that Jökulsárlón lagoon uptakes CO₂ at $0.19\text{--}1.14$ g CO₂ m⁻² d⁻¹ (Ljungberg et al., 2024) (Table S6 in Supporting Information S1). To evaluate their sustained global warming potential, we converted CH₄ and N₂O fluxes to CO₂-equivalent over 20 and 100 years timescales (Neubauer & Megonigal, 2019). The lagoon CO₂ uptake was up to 30 and 300 times higher than the CO₂-equivalent CH₄ and N₂O emissions, respectively (Table S7 in Supporting Information S1). Similarly, the direct CO₂ uptake in Iceland shelf waters (-0.5 g CO₂ m⁻² d⁻¹) was 60 times greater than combined CO₂-equivalent CH₄ and N₂O emissions in shelf (Jeansson et al., 2015). The strong CO₂ uptake capacity of cold waters largely counteracts the impact of CH₄-enriched glacial waters, highlighting the importance of high latitude oceans as net

sinks of greenhouse gases with a high potential for carbon sequestration despite enhanced CH₄ emissions (Borges et al., 2005; Olafsson et al., 2021; Pohlman et al., 2017).

5. Conclusions

We estimate CH₄ and N₂O emissions across a glacier-lagoon-shelf continuum during the summer. We found a large variability in greenhouse gas concentrations at the glacier front and glacier ponds where CH₄ could be lost due to oxidation (Dieser et al., 2014) and evasion from upstream sources (Burns et al., 2018). Ultimately, microbial processes, the magnitude of glacial discharge, water residence time, and upstream processes determine the sources and sinks of CH₄ and N₂O, and the fluxes to the atmosphere (Damm et al., 2010; Leonte et al., 2017; Rees et al., 2022). The larger shelf area relative to the lagoon compensates for smaller areal atmospheric greenhouse gas fluxes from shelf waters, making shelf waters much more important than the estuarine lagoon from a total flux perspective. The strong CO₂ uptake capacity of high-latitude oceans and marine terminating glacier areas suggests they will likely remain net greenhouse gas sinks despite large localized CH₄ sources and a very small N₂O source approaching background concentrations.

Data Availability Statement

Data on CH₄, N₂O and environmental variables used in this study are archived via Yau et al. (2025). Data on water flow, nutrient and carbonate system in Jökulsárlón Lagoon are available via Ljungberg et al. (2023). Atmospheric CH₄ and N₂O concentration are available from NOAA Global monitoring laboratory (<https://www.gml.noaa.gov/dv/site/index.php?stacode=ICE>). Ocean basemap was retrieved from Esri, GEBCO, NOAA, National Geographic, DeLorme, HERE, [Geonames.org](https://www.geonames.org), and other contributors.

Acknowledgments

We thank the crew of R/V Skagerak, and Shibin Zhao, Alex Cabral, Tibaud Cardis, Tobia Politi, Aprajita Singh Tomer and Markus Olsson for their outstanding support during the cruise. This project was partially funded by the Swedish Research Council Vetenskapsrådet (2019-03930, 2020-00457 and 2022-04710).

References

- Amorcho, J., & DeVries, J. J. (1980). A new evaluation of the wind stress coefficient over water surfaces. *Journal of Geophysical Research*, 85(C1), 433–442. <https://doi.org/10.1029/JC085iC01p00433>
- Björnsson, H., Pálsson, F., & Guðmundsson, S. (2001). Jökulsárlón at Breiðamerkursandur, Vatnajökull, Iceland: 20th century changes and future outlook. *Jökull Journal*, 50(1), 1–18. <https://doi.org/10.33799/jokull2001.50.001>
- Borges, A. V., Delille, B., & Frankignoulle, M. (2005). Budgeting sinks and sources of CO₂ in the coastal ocean: Diversity of ecosystems counts. *Geophysical Research Letters*, 32(14), 2005GL023053. <https://doi.org/10.1029/2005GL023053>
- Brandon, M., Hodgkins, R., Björnsson, H., & Ólafsson, J. (2017). Multiple melt plumes observed at the Breiðamerkjökull ice face in the upper waters of Jökulsárlón lagoon, Iceland. *Annals of Glaciology*, 58(74), 131–143. <https://doi.org/10.1017/aog.2017.10>
- Burns, R., Wynn, P. M., Barker, P., McNamara, N., Oakley, S., Ostle, N., et al. (2018). Direct isotopic evidence of biogenic methane production and efflux from beneath a temperate glacier. *Scientific Reports*, 8(1), 17118. <https://doi.org/10.1038/s41598-018-35253-2>
- Crabeck, O., Delille, B., Thomas, D., Geilfus, N.-X., Rysgaard, S., & Tison, J.-L. (2014). CO₂ and CH₄ in sea ice from a subarctic fjord under influence of riverine input. *Biogeosciences*, 11(23), 6525–6538. <https://doi.org/10.5194/bg-11-6525-2014>
- Damm, E., Bauch, D., Krumpfen, T., Rabe, B., Korhonen, M., Vinogradova, E., & Uhlig, C. (2018). The transpolar drift conveys methane from the Siberian Shelf to the central Arctic Ocean. *Scientific Reports*, 8(1), 4515. <https://doi.org/10.1038/s41598-018-22801-z>
- Damm, E., Helmke, E., Thoms, S., Schauer, U., Nothig, E., Bakker, K., & Kiene, R. P. (2010). Methane production in aerobic oligotrophic surface water in the central Arctic Ocean. *Biogeosciences*, 7(3), 1099–1108. <https://doi.org/10.5194/bg-7-1099-2010>
- Damm, E., Mackensen, A., Budéus, G., Faber, E., & Hanfland, C. (2005). Pathways of methane in seawater: Plume spreading in an Arctic shelf environment (SW-Spitsbergen). *Continental Shelf Research*, 25(12–13), 1453–1472. <https://doi.org/10.1016/j.csr.2005.03.003>
- Dieser, M., Broensen, E. L. J. E., Cameron, K. A., King, G. M., Achberger, A., Choquette, K., et al. (2014). Molecular and biogeochemical evidence for methane cycling beneath the western margin of the Greenland Ice Sheet. *The ISME Journal*, 8(11), 2305–2316. <https://doi.org/10.1038/ismej.2014.59>
- Fariás, L., Bello, E., Arancibia, G., & Fernandez, J. (2018). Distribution of dissolved methane and nitrous oxide in Chilean coastal systems of the Magellanic Sub-Antarctic region (50°–55°S). *Estuarine, Coastal and Shelf Science*, 215, 229–240. <https://doi.org/10.1016/j.ecss.2018.10.020>
- Fenwick, L., Capelle, D., Damm, E., Zimmermann, S., Williams, W. J., Vagle, S., & Tortell, P. D. (2017). Methane and nitrous oxide distributions across the North American Arctic Ocean during summer, 2015. *Journal of Geophysical Research: Oceans*, 122(1), 390–412. <https://doi.org/10.1002/2016JC012493>
- Frey, C., Tang, W., Ward, B. B., & Lehmann, M. F. (2024). Sample preservation methods for nitrous oxide concentration and isotope ratio measurements in aquatic environments. *Limnology and Oceanography: Methods*, 22(10), 771–788. <https://doi.org/10.1002/lom3.10638>
- Graly, J. A., Drever, J. I., & Humphrey, N. F. (2017). Calculating the balance between atmospheric CO₂ drawdown and organic carbon oxidation in subglacial hydrochemical systems. *Global Biogeochemical Cycles*, 31(4), 709–727. <https://doi.org/10.1002/2016GB005425>
- Harris, P. W. V. (1976). The seasonal temperature-salinity structure of a glacial lake: Jökulsárlón, South-East Iceland. *Geografiska Annaler*, 58(4), 329. <https://doi.org/10.2307/520538>
- Hawkins, J. R. (2021). Trickle and treat? The critical role of marine-terminating glaciers as icy macronutrient pumps in Polar Regions. *Journal of Geophysical Research: Biogeosciences*, 126(10), e2021JG006598. <https://doi.org/10.1029/2021JG006598>
- Hopwood, M. J., Carroll, D., Dunse, T., Hodson, A., Holding, J. M., Iriarte, J. L., et al. (2020). Review article: How does glacier discharge affect marine biogeochemistry and primary production in the Arctic? *The Cryosphere*, 14(4), 1347–1383. <https://doi.org/10.5194/tc-14-1347-2020>
- IMO. (2024). Icelandic meteorological office. Retrieved from <https://en.vedur.is/weather/stations/?s=kvisk>
- Jeansson, E., Bellerby, R. G. J., Skjelvan, I., Frigstad, H., Ólafsdóttir, S. R., & Ólafsson, J. (2015). Fluxes of carbon and nutrients to the Iceland Sea surface layer and inferred primary productivity and stoichiometry. *Biogeosciences*, 12(3), 875–885. <https://doi.org/10.5194/bg-12-875-2015>

- Kitidis, V., Upstill-Goddard, R. C., & Anderson, L. G. (2010). Methane and nitrous oxide in surface water along the North-West Passage, Arctic Ocean. *Marine Chemistry*, 121(1–4), 80–86. <https://doi.org/10.1016/j.marchem.2010.03.006>
- Kleber, G. E., Hodson, A. J., Magerl, L., Mannerfelt, E. S., Bradbury, H. J., Zhu, Y., et al. (2023). Groundwater springs formed during glacial retreat are a large source of methane in the high Arctic. *Nature Geoscience*, 16(7), 597–604. <https://doi.org/10.1038/s41561-023-01210-6>
- Kochitzky, W., & Copland, L. (2022). Retreat of Northern Hemisphere marine-terminating glaciers, 2000–2020. *Geophysical Research Letters*, 49(3), e2021GL096501. <https://doi.org/10.1029/2021GL096501>
- Lamarche-Gagnon, G., Wadham, J. L., Sherwood Lollar, B., Arndt, S., Fietzek, P., Beaton, A. D., et al. (2019). Greenland melt drives continuous export of methane from the ice-sheet bed. *Nature*, 565(7737), 73–77. <https://doi.org/10.1038/s41586-018-0800-0>
- Lan, X., Thoning, K. W., & Dlugokencky, E. J. (2023). Trends in globally-averaged CH₄, N₂O, and SF₆ determined from NOAA global monitoring laboratory measurements (version 2023-10). <https://doi.org/10.1513/P8XG-AA10>
- Leonte, M., Kessler, J. D., Kellermann, M. Y., Arrington, E. C., Valentine, D. L., & Sylva, S. P. (2017). Rapid rates of aerobic methane oxidation at the feather edge of gas hydrate stability in the waters of Hudson Canyon, US Atlantic Margin. *Geochimica et Cosmochimica Acta*, 204, 375–387. <https://doi.org/10.1016/j.gca.2017.01.009>
- Ljungberg, W., Yau, Y. Y., Cabral, A., Majtényi-Hill, C., Henriksson, L., McKenzie, T., et al. (2023). Carbon outwelling and uptake along a tidal glacier-lagoon-ocean continuum (1.0) [Dataset]. *Zenodo*. <https://doi.org/10.5281/zenodo.10077831>
- Ljungberg, W., Yau, Y. Y., Cabral, A., Majtényi-Hill, C., Henriksson, L., McKenzie, T., et al. (2024). Carbon outwelling and uptake along a tidal glacier-lagoon-ocean continuum. *Journal of Geophysical Research: Biogeosciences*, 129(6), e2023JG007895. <https://doi.org/10.1029/2023JG007895>
- Logemann, K., Ólafsson, J., Snorrason, Á., Valdimarsson, H., & Marteinsdóttir, G. (2013). The circulation of Icelandic waters – A modelling study. *Ocean Science*, 9(5), 931–955. <https://doi.org/10.5194/os-9-931-2013>
- Manning, C. C. M., Zheng, Z., Fenwick, L., McCulloch, R. D., Damm, E., Izett, R. W., et al. (2022). Interannual variability in methane and nitrous oxide concentrations and sea-air fluxes across the North American Arctic Ocean (2015–2019). *Global Biogeochemical Cycles*, 36(4), e2021GB007185. <https://doi.org/10.1029/2021gb007185>
- Meire, L., Paulsen, M. L., Meire, P., Rysgaard, S., Hopwood, M. J., Sejr, M. K., et al. (2023). Glacier retreat alters downstream fjord ecosystem structure and function in Greenland. *Nature Geoscience*, 16(8), 671–674. <https://doi.org/10.1038/s41561-023-01218-y>
- Neubauer, S. C., & Megonigal, J. P. (2019). Correction to: Moving beyond global warming potentials to quantify the climatic role of ecosystems. *Ecosystems*, 22(6), 1931–1932. <https://doi.org/10.1007/s10021-019-00422-5>
- Ólafsson, J., Ólafsdóttir, S. R., Takahashi, T., Danielsen, M., & Arnarson, T. S. (2021). Enhancement of the North Atlantic CO₂ sink by Arctic Waters. *Biogeosciences*, 18(5), 1689–1701. <https://doi.org/10.5194/bg-18-1689-2021>
- Overeager, I., Hudson, B. D., Syvitski, J. P. M., Mikkelsen, A. B., Hasholt, B., Van Den Broeke, M. R., et al. (2017). Substantial export of suspended sediment to the global oceans from glacial erosion in Greenland. *Nature Geoscience*, 10(11), 859–863. <https://doi.org/10.1038/ngeo3046>
- Pain, A. J., Martin, J. B., Martin, E. E., Rennermalm, Å. K., & Rahman, S. (2021). Heterogeneous CO₂ and CH₄ content of glacial meltwater from the Greenland Ice Sheet and implications for subglacial carbon processes. *The Cryosphere*, 15(3), 1627–1644. <https://doi.org/10.5194/tc-15-1627-2021>
- Pohlman, J. W., Greinert, J., Ruppel, C., Silyakova, A., Vielstädte, L., Casso, M., et al. (2017). Enhanced CO₂ uptake at a shallow Arctic Ocean seep field overwhelms the positive warming potential of emitted methane. *Proceedings of the National Academy of Sciences*, 114(21), 5355–5360. <https://doi.org/10.1073/pnas.1618926114>
- Randall, K., Scarratt, M., Levasseur, M., Michaud, S., Xie, H., & Gosselin, M. (2012). First measurements of nitrous oxide in Arctic sea ice. *Journal of Geophysical Research*, 117(C9), 2011JC007340. <https://doi.org/10.1029/2011JC007340>
- R Core Team. (2021). R: Language and environment for statistical computing [Computer software]. *R Core Team*. <https://www.gbif.org/tool/81287/r-a-language-and-environment-for-statistical-computing>
- Rees, A. P., Bange, H. W., Arévalo-Martínez, D. L., Artioli, Y., Ashby, D. M., Brown, I., et al. (2022). Nitrous oxide and methane in a changing Arctic Ocean. *Ambio*, 51(2), 398–410. <https://doi.org/10.1007/s13280-021-01633-8>
- Rees, A. P., Brown, I. J., Jayakumar, A., Lessin, G., Somerfield, P. J., & Ward, B. B. (2021). Biological nitrous oxide consumption in oxygenated waters of the high latitude Atlantic Ocean. *Communications Earth & Environment*, 2(1), 36. <https://doi.org/10.1038/s43247-021-00104-y>
- Repeta, D. J., Ferrón, S., Sosa, O. A., Johnson, C. G., Repeta, L. D., Acker, M., et al. (2016). Marine methane paradox explained by bacterial degradation of dissolved organic matter. *Nature Geoscience*, 9(12), 884–887. <https://doi.org/10.1038/ngeo2837>
- Schuler, K. H., & Tortell, P. D. (2023). Impacts of vertical mixing and ice-melt on N₂O and CH₄ concentrations in the Canadian Arctic Ocean. *Continental Shelf Research*, 269, 105124. <https://doi.org/10.1016/j.csr.2023.105124>
- Sparrow, K. J., Kessler, J. D., Southon, J. R., Garcia-Tigeros, F., Schreiner, K. M., Ruppel, C. D., et al. (2018). Limited contribution of ancient methane to surface waters of the U.S. Beaufort Sea shelf. *Science Advances*, 4(1), eaao4842. <https://doi.org/10.1126/sciadv.aao4842>
- Stibal, M., Wadham, J. L., Lis, G. P., Telling, J., Pancost, R. D., Dubnick, A., et al. (2012). Methanogenic potential of Arctic and Antarctic subglacial environments with contrasting organic carbon sources. *Global Change Biology*, 18(11), 3332–3345. <https://doi.org/10.1111/j.1365-2486.2012.02763.x>
- St. Pierre, K. A., St. Louis, V. L., Schiff, S. L., Lehnher, I., Dainard, P. G., Gardner, A. S., et al. (2019). Proglacial freshwaters are significant and previously unrecognized sinks of atmospheric CO₂. *Proceedings of the National Academy of Sciences*, 116(36), 17690–17695. <https://doi.org/10.1073/pnas.1904241116>
- Stroeve, J. C., Markus, T., Boisvert, L., Miller, J., & Barrett, A. (2014). Changes in Arctic melt season and implications for sea ice loss. *Geophysical Research Letters*, 41(4), 1216–1225. <https://doi.org/10.1002/2013GL058951>
- Thamdrup, B., Steinsdóttir, H. G. R., Bertagnolli, A. D., Padilla, C. C., Patin, N. V., Garcia-Robledo, E., et al. (2019). Anaerobic methane oxidation is an important sink for methane in the ocean's largest oxygen minimum zone. *Limnology & Oceanography*, 64(6), 2569–2585. <https://doi.org/10.1002/lno.11235>
- Thornton, B. F., Prytherch, J., Andersson, K., Brooks, I. M., Salisbury, D., Tjernström, M., & Crill, P. M. (2020). Shipborne eddy covariance observations of methane fluxes constrain Arctic sea emissions. *Science Advances*, 6(5), eaay7934. <https://doi.org/10.1126/sciadv.aay7934>
- Tsubouchi, T., Våge, K., Hansen, B., Larsen, K. M. H., Østerhus, S., Johnson, C., et al. (2021). Increased ocean heat transport into the Nordic Seas and Arctic Ocean over the period 1993–2016. *Nature Climate Change*, 11(1), 21–26. <https://doi.org/10.1038/s41558-020-00941-3>
- USGS. (2019). NASA Earth Observatory image using Landsat 8 data. Retrieved from <https://landsat.visibleearth.nasa.gov/view.php?id=145984>
- Verdugo, J., Damm, E., Schaffer, J., Bauch, D., Meyer, H., & Kaiser, J. (2022). Impacts of glacier and sea ice melt on methane pathways on the Northeast Greenland shelf. *Continental Shelf Research*, 243, 104752. <https://doi.org/10.1016/j.csr.2022.104752>

- Voytenko, D., Dixon, T. H., Howat, I. M., Gourmelen, N., Lembke, C., Werner, C. L., et al. (2015). Multi-year observations of Breiðamerkurjökull, a marine-terminating glacier in southeastern Iceland, using terrestrial radar interferometry. *Journal of Glaciology*, 61(225), 42–54. <https://doi.org/10.3189/2015JoG14J099>
- Wadham, J. L., Hawkings, J. R., Tarasov, L., Gregoire, L. J., Spencer, R. G. M., Gutjahr, M., et al. (2019). Ice sheets matter for the global carbon cycle. *Nature Communications*, 10(1), 3567. <https://doi.org/10.1038/s41467-019-11394-4>
- Wanninkhof, R. (2014). Relationship between wind speed and gas exchange over the ocean revisited. *Limnology and Oceanography: Methods*, 12(6), 351–362. <https://doi.org/10.4319/lom.2014.12.351>
- Weiss, R. F., & Price, B. A. (1980). Nitrous oxide solubility in water and seawater. *Marine Chemistry*, 8(4), 347–359. [https://doi.org/10.1016/0304-4203\(80\)90024-9](https://doi.org/10.1016/0304-4203(80)90024-9)
- Wiesenburg, D. A., & Guinasso, N. L. (1979). Equilibrium solubilities of methane, carbon monoxide, and hydrogen in water and sea water. *Journal of Chemical & Engineering Data*, 24(4), 356–360. <https://doi.org/10.1021/jc60083a006>
- Wilson, S. T., Bange, H. W., Arévalo-Martínez, D. L., Barnes, J., Borges, A. V., Brown, I., et al. (2018). An intercomparison of oceanic methane and nitrous oxide measurements. *Biogeosciences*, 15(19), 5891–5907. <https://doi.org/10.5194/bg-15-5891-2018>
- Yau, Y. Y., Ljungberg, W., Cheung, H. L. S., McKenzie, T., Henriksson, L., Majtényi-Hill, C., et al. (2025). Combined CH₄, N₂O and CO₂ fluxes budgets reveal a net carbon sink across a glacier-ocean continuum (Version v3) [Dataset]. *Zenodo*. <https://doi.org/10.5281/zenodo.13374162>
- Zhang, J., Zhan, L., Chen, L., Li, Y., & Chen, J. (2015). Coexistence of nitrous oxide undersaturation and oversaturation in the surface and subsurface of the western Arctic Ocean. *Journal of Geophysical Research: Oceans*, 120(12), 8392–8401. <https://doi.org/10.1002/2015JC011245>
- Pórarinnsson, Ó., & Hróðmarsson, H. B. (2022). Rennslismælingar í Jökulsá á Breiðamerkursandi (OTh/HBH/2022-01).
- Pórarinnsson, Ó., Reynisson, N. F., & Hróðmarsson, H. B. (2020). Rennslismælingar í Jökulsá á Breiðamerkursandi [ÓTh/ofl/2020-02].